PRELIMINARY ASSESSMENT OF A WARPING WING CONFIGURATION IN ROLLING CONTROL

Cestino E.*, Frulla G.*, Lanzillotti A.*
***Politecnico di Torino, Dept Mechanical and Aerospace Eng. (DIMEAS)**

Keywords: *morphing, warping, optimization*

Abstract

The preliminary analysis and the possible advantages of a morphing solution replacing the traditional hinged aileron configuration has been analyzed in order to evaluate its energy efficiency in UAV configurations with limited payload capacity and power available for flight. The parameters considered are the wing aspect ratio, the torsional stiffness, the position and the aileron deflection and the consequent actuation rib rotation in the morphing solution. The analysis showed that the morphing solution is very advantageous in all cases requiring high rolling moments with a more evident advantage at high aspect ratios. The traditional solution still remain advantageous at low aspect ratios and low rolling moments.

1. Introduction

The concept of morphing wing dates back to the first wright brothers' airplane but the development of new materials and technologies and consequent possible increase in performance has renewed interest even today. Several adaptive wings concepts of varying complexity were investigated with regard to specific applications and objectives [1,9]. The idea to control twist angle variations along a large part of the wing span may represent a valid strategy to overcome the drawbacks of aileron-based control in high-aspect-ratio wings. Pecora et Al. [2] presents a numerical investigations that analyze the advantages of an unconventional roll control strategy based on wing twist morphing applied to a commercial sailplane. Ajaj et al. [3] shown a feasibility study of the adaptive torsion wing applied to a MALE-UAV. The use of a set of torque rods, aligned along the wings, are presented by Abdulrahim et Al. [4] and used to twist a membrane wing of a MAV-UAV and a static aeroelastic model of the micro air vehicle is developed and validated to optimize the performance of the torque-actuated wing structure in [5]. A possible solution for adaptive wing configuration can be found in the VENTURAS Project idea [6,7].

2. Aeroelastic model and optimization code

This section will give an overview of the global aeroelastic optimization code, developed in order to evaluate potential advantages in the implementation of wing morphing technologies, as well as an in depth illustration of its core aerodynamic and structural components, emphasizing spectrum of applicability and current limitations.

The objective of this study is to evaluate the potential advantages in the adoption of wing warping mechanisms, as a means of producing rolling moment, in opposition to the currently adopted hinged ailerons. The study will be conducted with both an ideally rigid structure and an increasingly more flexible structure, emphasizing the impact the latter has on the theoretical rigid results, whilst varying the aspect ratio of the wing in exam. An aileron wing model will be used both as a constraint and reference case (as indicated in **Table 1**) for each studied cases (see **Table 2**), defined solely by torsional stiffness and aspect ratio, both lift and drag spanwise distributions will be calculated by an aeroelastic code at different aileron angles (variable in a range between 2° and 10°), thus properly grasping the performance of an

equivalent warping wing in a full operational spectrum. The aileron lift and drag contributions will be used to compute the required reference power and the rolling moment produced (this constraint value must be satisfied by the morphing option in the same operating conditions). In all the cases examined, the hypothesis adopted was that the actuation power required to the configuration with aileron is equal for the warping case.

Table 1 Constant parameters	
Profile	NACA 4412
α_0	-0.076 rad
2D Lift slope (CLα) @ Re=1.28E6	6.08
Wing chord length	0.5 m
Relative Airspeed	30 m/s
Air density and viscosity	Sea Level Conditions
Aerodynamic axis relative position	25% chord length
Elastic axis relative position	50% chord length
Total weight	15 kg

The problem analysis is structured in two main phases: a cruise point phase, conducted for each case study, and an optimization and final morphing evaluation phase, as shown in **Figure 1**. The first phase is necessary as to fix the starting point from which to evaluate the roll maneuver at leveled flight conditions. In particular the angle of attack will be susceptible to both aspect ratio and torsional stiffness. The first influences the angle of attack α through a variation in wing surface (having chosen a constant wing chord and flight speed) and C_{L_α} parameter, the latter introduces a variation in the local angle of attack as a result of elastic wing torsion, effectively increasing the total wing C_L compared to a rigid wing. A series of aspect ratio (see **Table 2**) values has been chosen in order to study different vehicle categories.

Table 2 Case studies						
	q/qd			**q/qd**		
	rig	0.1	0.2	rig	0.1	0.2
AR	**GJ [kgm^2]**			**α_{trim} [°]**		
6	∞	1923.25	961.63	3.321	3.196	3.071
16	∞	13676.46	6838.23	1.048	0.998	0.948
26	∞	36114.41	18057.20	0.615	0.584	0.552

For each case different values of torsional stiffness *GJ* have been assigned to evaluate the impact of varying the aeroelastic parameters, q/q_D where q is the cruise condition dynamic pressure and q_D is the the dynamic pressure at divergence condition. Maintaining constant the q value different q/q_D means different degree of wing flexibility and the corresponding *GJ* value is obtained by **eq 17**. The second phase consists in the determination of the performance of an aileron wing configuration flying in the above cruise conditions, taking into account the appropriate torsional stiffness for each case. This is executed for a range of aileron angles to fully comprehend how a warping wing compares in a realistic operational environment and how many degrees of freedom (actuation ribs rotation and span position) are effectively involved in the actuation of the rolling command in its full range.

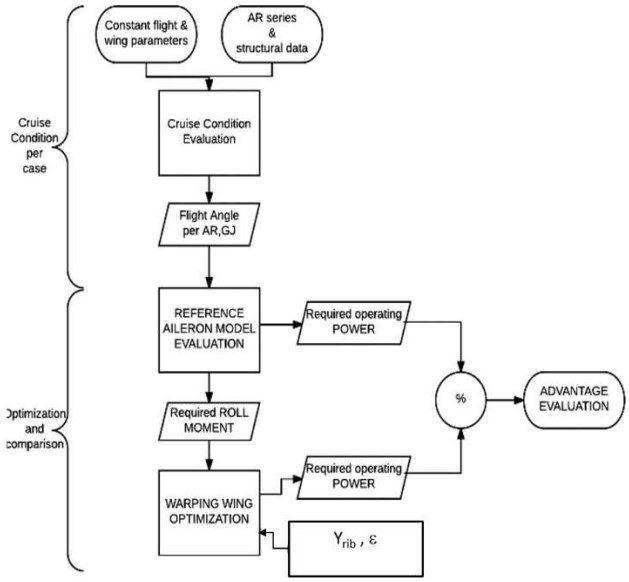

Figure 1 Analysis workflow

The aileron model, other than being a performance reference point, acts as a constraint for the optimization of the warping wing counterpart: the warping wing must produce the same rolling moment at fixed flight condition for each aileron angle.
This constraint allows to obtain a wing configuration easily adaptable to already existing aircraft with comparable roll performance, without requiring a redesign from the point of view of flight mechanics.

2.1. Aerodynamic model

In order to calculate the lift and drag spanwise distributions, inherently asymmetrical due to the nature of the problem in exam, Prandtl's lifting line theory has been used. Although more robust aerodynamic analysis solutions could be implemented, a reduced order model is a good starting point for a preliminary analysis and can be easily and effectively adapted to both an aileron and warping wing, as well as being easily coupled with the structural code and the optimization code. The aerodynamic distributions in leveled flight conditions are calculated starting with the characterization of the profile at current Reynolds number. Having imposed ambient conditions, velocity and chord length as constants in this parametric study, the Reynolds value is constant along the span. The base, positive and negative aileron angle profiles are fully characterized through the use of XFOIL and the resulting two-dimensional aerodynamic behavior in terms of C_L C_D C_M determined. The wing is then discretized with a spanwise cosine distribution mesh, necessary to properly calculate the 3-dimensional aerodynamic effects near the wingtips. To each node a local angle of attack α_{loc} is assigned and calculated as

$$\alpha_{loc}(i) = [\alpha_{trim} - \alpha_0(i) - \alpha_{in}(i)] + \epsilon(i) + \theta(i) \quad (1)$$

where α_{trim} is constant along the span and defined by the flight condition, $\alpha_0(i)$ is the zero lift angle of attack related to the chosen airfoil geometry and varies only at those nodes representing the aileron profiles and are thus limited to only the aileron extension, $\alpha_{ind}(i)$ is the tip vortices induced angle, $\epsilon(i)$ is the local profile rotation introduced by the warping mechanism and $\theta(i)$ is the airfoil rotation introduced by aeroelastic phenomena, initially considered null and iterated until convergence is reached. A generic lift distribution can be approximated through an expansion in series of trigonometric functions, we are able to calculate the local circuitation (as from Prantl's theory) as

$$\Gamma(\Theta) = 2bV_\infty \sum_{n=1}^{\infty} A_n \sin(n\Theta) \quad (2)$$

Where $\Theta = (0, \pi)$ is a lineary spaced vector of angles describing the local node as

$$y(i) = \frac{b}{2}\cos(\Theta) \quad (3)$$

Replacing **1.2** in Prantl's integrodifferential equation and assuming a rectangular wing of aspect ratio λ=b/c, we obtain a system of equations in the unknown variables A_n

$$\sum_{n=1}^{\infty} A_n \sin(n\Theta)\left[\frac{4\lambda}{C_{L_\alpha}} + \frac{n}{\sin(\Theta)}\right] = \alpha_{loc}(\Theta) \quad (4)$$

Obtained the solution from system **eq 4** and substituting the values in **eq 2** we obtain a vector of Γ values at each node, from which we can calculate the local lift and C_L coefficient through

$$L(\Theta) = \rho V_\infty \Gamma(\Theta)$$
$$C_L(\Theta) = \frac{L(\Theta)}{\frac{1}{2}\rho V_\infty c} \quad (5)$$

The corresponding induced angle of attack and drag coefficient is then computed by

$$\alpha_{induced}(i) = \frac{C_L(i)}{C_{L_\alpha}(i)} - \alpha_{loc}(i)$$
$$C_{D_{induced}}(i) = C_L(i) * \alpha_{induced}(i) \quad (6)$$

From the spanwise C_L distribution, the pressure and friction drag C_D and sectional pitching moment C_M are recovered by the 2D airfoil computation. . It is then possible to calculate the different wing coefficients as

$$C_{L,D,M_{wing}} = \frac{\int_{-\frac{b}{2}}^{\frac{b}{2}} C_{L,D,M}(y) * c \, dy}{S} \quad (7)$$

In particular, in order to evaluate the angle of attack in leveled flight conditions from which to initiate the rolling maneuver, for each case study C_L-α behaviors are diagrammed and the 3-dimensional C_{L_α} is extrapolated through interpolation. The angle of attack (α_{trim}) is then

simply obtained imposing translational equilibrium (lift=weight) through the z-axis, in particular, the weight is considered constant throughout all the cases studied. Having found the appropriate α_{trim} value for each case study, it is then possible to compute the rolling moment and required flight power for both aileron and warping wing configurations by:

$$M_{roll} = \int_{-b/2}^{b/2} L(y) * y \, dy \qquad (8)$$

$$Power = \frac{1}{2}\rho V_{\infty}^{3} S C_{D_{TOT}}$$

Where $C_{D_{TOT}} = C_D + C_{Di}$.

These distributions are then passed on to the structural code, which in turn outputs $\theta(i)$ and the process iterates until convergence is met.
The workflow is summarized in **Figure 2**

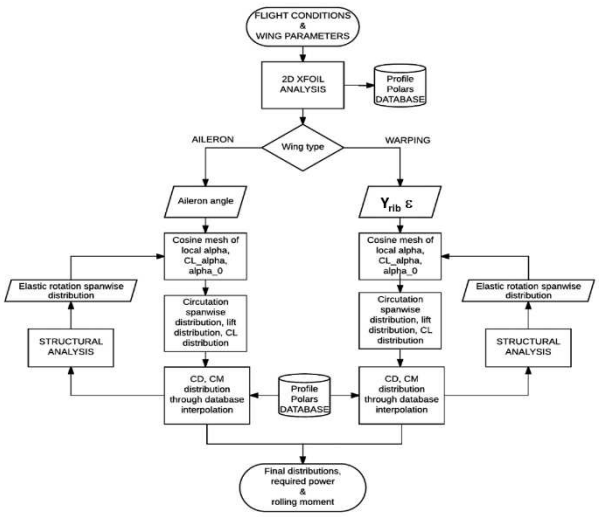

Figure 2 Aerodynamic workflow

The wing types analyzed and compared in this study are defined as follows:
AILERON-This wing, as shown in figure 3, is characterized by two aileron profiles positioned symmetrically in respect of the root profile of extension fixed at 20% of the semi wing span and starting point fixed at 70% of the semi span. The aileron profile is treated as a base profile with an hinge located at 80% of the chord length and at 50% of the local thickness. As described above, all the nodes that fall in this region of the wing are assigned the appropriate α_0 and C_{L_α} values and the resulting C_D and C_M values are extrapolated from the according airfoil polars.

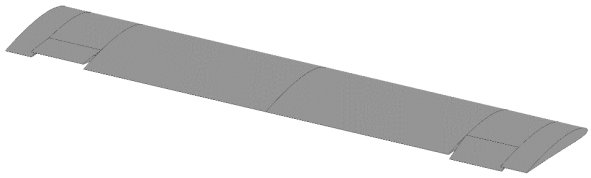

Figure 3 Aileron wing

WARPING-This wing is characterized by a constant profile linearly rotated from the root with a gradient defined by the semi-spanwise position and rotation of the actuator rib and a constant rotation angle from this point outwards (see figure 4). This is antisymmetrically repeated on the opposite half of the wing. Positive profile rotations are induced on the right wing to achieve negative roll about the x-axis of the plane.

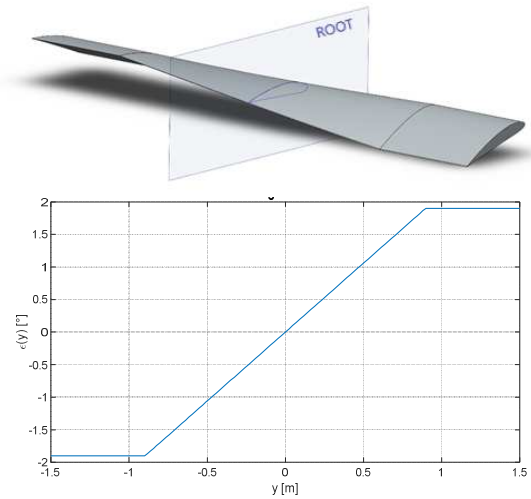

Figure 4 Warping wing

2.2. Structural model

The aerodynamic model alone treats the wing as a rigid body and thus needs to be interfaced with a structural model that lets us capture the aeroelastic effects on the wing. This is essential for a more realistic evaluation of the possible advantages introduced by the warping wing in respect of the conventional aileron wing. Being the rotation of the ribs the sole method of production of rolling moment in the warping wing, a structure with torsional rotation as single degree of freedom has been implemented even if

the wing will also bend under the application of an aerodynamic load.

The structural model is called from the aerodynamic function at each iteration, as shown in Errore. L'origine riferimento non è stata trovata.**.** It receives in input the node mesh and relative aerodynamic coefficients distributions from which to calculate the aerodynamic loads acting on the structure and outputs in return the rotational elastic displacements at each node, that are subsequently added in the aerodynamic analysis in eq. **1**. For a first approach to the subject, the structural flexibility is limited only to the spar of the wing (both ribs and skin are not considered at this point), and the torsional stiffness *GJ* is considered constant throughout the wing. The rotational equilibrium equation is indicated in **eq 9** and numerically solved through the use of linear finite elements method. It is calculated as

$$-GJ\frac{d}{dy}\left(\frac{d\theta}{dy}\right) = t(y) \qquad (9)$$

where *t(y)* are the external torques applied on the structured defined as

$$t(y) = \frac{1}{2}\rho V_\infty^2 (ecC_L + c^2 C_M) \qquad (10)$$

It is assumed that the elastic axis and the line of centers of mass are collinear, meaning that mass distributions are not dealt with in this analysis but can be easily implemented for future studies. Forces are applied on the aerodynamic line positioned on the first quarter of the profile chord as from Prandtl's theory, and induce a torque on the structure through the distance e from the elastic axis. The wing is split in its two semispans and boundary condition on the root and tip stations will be applied as $\theta(root) = 0$ and $\frac{d\theta}{dy}(tip) = 0$.

The structural behavior of the wing is approximated by means of Finite Element approach. The wing is reduced to its elastic axis with known properties and it is subdivided in N=200 monodimensional two nodes elements reducing the problem to a system of linear equations in the unknown variables θ_i as indicated in:

$$[K]\{\theta\} = \{f\} \qquad (11)$$

Where $[K]$ is the wing structure stiffness matrix and $\{f\}$ is the vector of generalized nodal loads and $\{\theta\}$ is the vector of generalized nodal displacements. Starting from the definition of the generic torsional element stiffness matrix:

$$[K_j] = \frac{(GJ)_j}{l_j}\begin{bmatrix} 1 & -1 \\ -1 & 1 \end{bmatrix} \qquad (12)$$

the classical assembling procedure has been adopted to obtain the entire structure stiffness matrix:

$$\begin{matrix} k_{11}^j & k_{12}^j & 0 & 0 \\ k_{12}^j & k_{22}^j + k_{11}^{j+1} & k_{12}^{j+1} & 0 \\ 0 & k_{12}^{j+1} & k_{22}^{j+1} + \cdots & 0 \\ 0 & 0 & 0 & \ldots \end{matrix} \qquad (13)$$

The nodal loads vector is derived considering constant chord elements and concentrated parameters approach

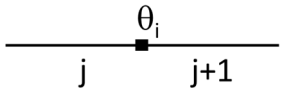

$$f_i = t(y_i)\frac{l_j + l_{j+1}}{2} \quad j = 1, \ldots, N$$
$$= t\left(\frac{b}{2}\right)\frac{l_{N+1}}{2} \quad j = N+1 \qquad (14)$$

Where j is the generic element and i the generic node.

Combining the solutions for the right and left wing, vector θ is obtained and can be subsequently dealt with in the aerodynamic model. The process iterates until the overwhole displacement reaches convergence at a user defined tolerance.

2.3. Optimization model

For a proper evaluation of the warping wing option, its characteristics need to be optimized as to satisfy rolling performances constrains and to

minimize the global required flight power, otherwise aiming to minimize the global drag coefficient. As shown in **Figure 2,** for each case study defined by torsional stiffness and aspect ratio, a range of aileron angles has been calculated in order to grasp a possible full operational range; each aileron angle performance is then compared to the results of the optimization for said particular case. This allows for a per case optimization, main conceptual reason for adopting morphing technologies, and emphasizes the effective degrees of freedom involved in the actuation for possible future implementations. Defined $\boldsymbol{x}$ the solution vector as

$$\boldsymbol{x} = \begin{Bmatrix} y \\ \epsilon \end{Bmatrix} \tag{15}$$

where y is the position of the actuator rib on the semiwing span and ε is its rotation.
The optimization problem is structured as follows:

$$\min Power(\boldsymbol{x})$$

$$s.t. \quad \begin{cases} M(\boldsymbol{x}) - M_{aileron} = 0 \\ \begin{Bmatrix} k \\ 0 \end{Bmatrix} \leq \boldsymbol{x} \leq \begin{Bmatrix} \frac{b}{2} - k \\ e_{max} = 8 \end{Bmatrix} \end{cases} \tag{16}$$

The lower and upper bounds for the solution have been chosen in order to allow for enough installation space of possible actuators near the root and tip ribs and to limit the rotation of the rib to angles where the aerodynamical model is still applicable and will not enter regions of stall that are not accounted for. MATLAB's built in optimizations suite (fmincon function-interior point gradient algorithm) has been used to evaluate optimal solutions for **eq.16**.

3. Results

The results obtained from the aeroelastic analysis and optimization were computed for the constant parameters :The case studies and relative torsional stiffness and cruise trim angle of attack α are illustrated in **Table .**
Each GJ value has been calculated in order to satisfy the percentage of torsional divergence dynamic pressure selected. Starting from

$$\frac{q}{q_D} = value$$
$$q_D = \left(\frac{\pi}{b}\right)^2 \left(\frac{GJ}{ceC_{L_\alpha}}\right) \tag{17}$$

GJ can be derived as

$$GJ = \frac{\frac{1}{2}\rho V_\infty^2}{\left(\frac{q}{q_D}\right)} ceC_{L_\alpha} \left(\frac{b}{\pi}\right)^2 \tag{18}$$

and the relative α_{trim} value can be determined imposing cruising conditions for a given aircraft weight. For each case study a series of aileron angles has been analyzed in the reference model and compared with the warping option as a means of inducing rolling moment. The effectiveness of the warping option is evaluated as a percentage of consumed ΔPower between rolling and cruising state defined as

$$\Delta P_{\%} = \frac{\Delta P_{morp} - \Delta P_{aileron}}{\Delta P_{aileron}} \tag{19}$$

Negative $\Delta P_{\%}$ indicate a reduction of required power to execute the maneuver and thus pose the warping option as the more efficient actuation method.
In **Figure 5** the constraint in terms of rolling moment that should be satisfied by the warping configuration has been indicated, as an example, for three values of wing aspect ratio and for the rigid case. In the subsequent study different flexibility levels are considered and constraint rolling moment updated accordingly.

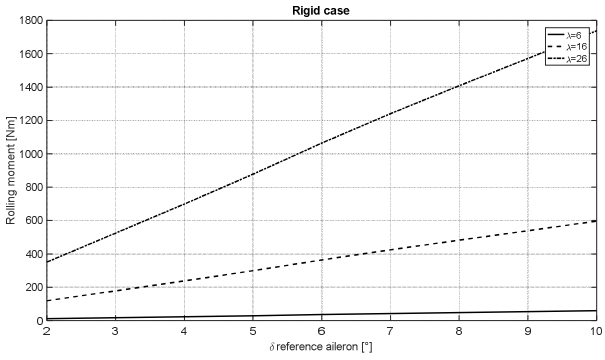

Figure 5 Rolling moments constraints

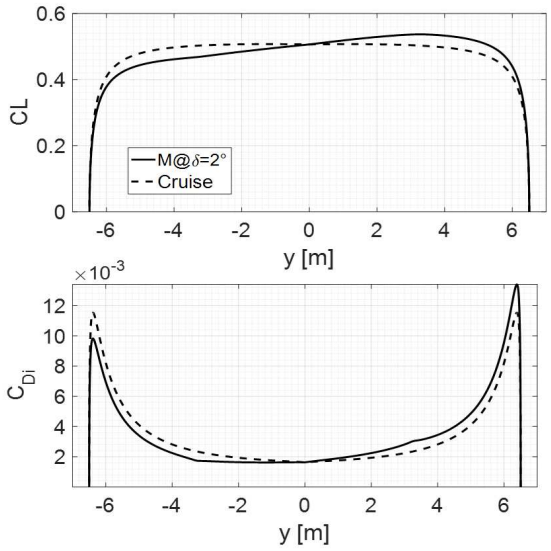

Figure 6 Rolling moments constraints: lift distribution

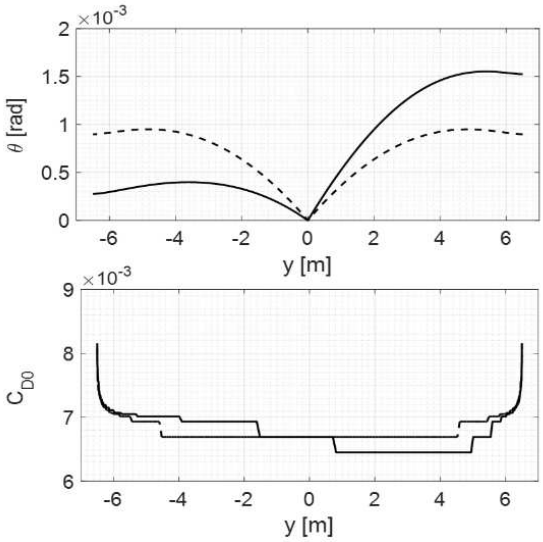

Figure 7 Rolling moments constraints: drag distribution

The $\Delta P_{\%}$ trends are diagrammed in **Figure** for the studied cases.

Figure 6 shows the lift distribution when the morphing wing is called to generate a specific roll moment respect to the cruise condition. **Figure 7** shows instead the trend of the elastic rotation and of the drag coefficient in the case of cruising and in the case with active morphing.

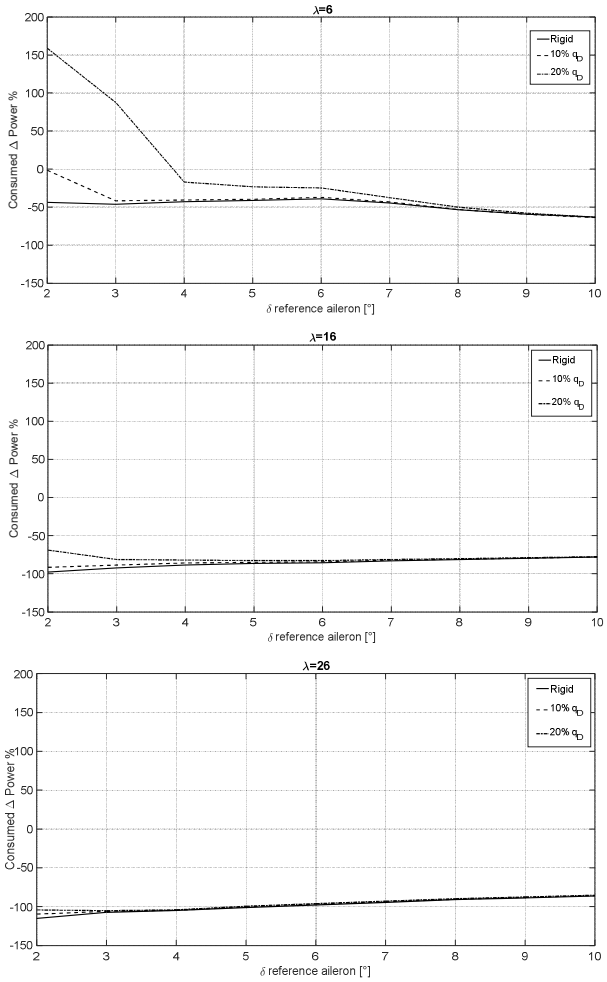

Figure 8 Advantage evalutation

It is possible to note that the warping option is particularly effective when called to induce high rolling moments: having defined the aileron extension as a fixed percentage of the semispan length, increasing aspect ratio wing induce a bigger rolling moment (**Figure**) and the warping option globally seems to be more effective in such conditions.

The $\Delta P_{\%}$ trends also underline a tendency to reduce the effectiveness of the warping option for increasingly more flexible structures. This is due to the intrinsic flexibility and the corresponding torsional angle θ that on one semiwing helps the positive rotation of the actuation rib ε and on the other semiwing contrasts the negative ε shifting the roll moment production on the semispan where ε and θ show the same sign.

The difference from rigid and flexible case in the region at low delta values, can be justified by the different method of production the rolling moment that in one case (aileron solution) is obtained by a small local variation of the aerodynamic characteristics while, in the morphing case, it is realized by a global variation of the characteristics. This produce in turn, a flexibility disturbance that affects a larger part of the wing making the aileron option still a viable solution as indicated in **Figure 8**.

At high delta values the effect of flexibility can be considered a secondary effect respect to the drag increase produced by the aileron deflection and the morphing solution seem to be the optimal.

For the highest aspect ratio the $\Delta P_{\%}$ reach values around -100% that are justified because the eps angle in the warping solution is very low and the power increment respect to the cruise condition to produce the required rolling moment is practically negligible always making the morphing solution very favorable.

Moving on to the analysis of the optimal position for the variables *y* and ε, it is possible to notice a tendency to limit the degree of freedom to the only rotation of the actuator rib for low aspect ratios . This tendency is lost with very high aspect ratios where the rolling moments that the wing is called to satisfy are of higher magnitude and the second degree of freedom can be used to further enhance the warping effectiveness (**Figure**).
In the maps shown in **Figure 10** and **11** the level curves represent the ΔP_{morph} respect to the cruise condition to obtain a particular rolling moment in the morphing solution. The dashed curves are the moment constraints and the optimal solution can only be found on this curves to respect the imposed moment constraint. The continuous line represents the locus of optimal solutions. It can be noted that when the momentum curves are parallel to the y axis, the degree of freedom related to the position of the actuation rib (y) is irrelevant for the generation of the moment. If the iso-moment curves exhibit a trend very similar to that of iso-power, then this will mean that choosing to fix a degree of freedom has little influence on the optimal result

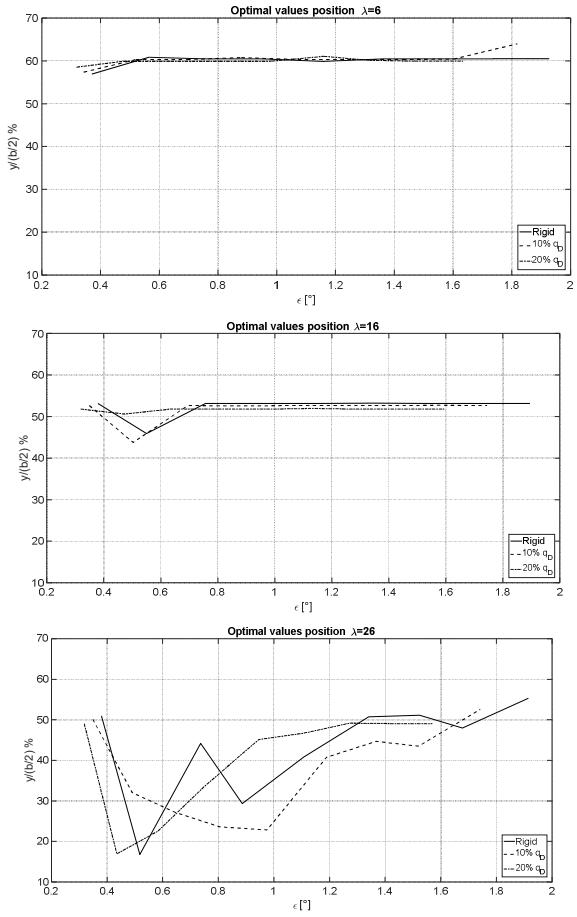

Figure 9 Optimal values trends

In the case of low AR it is clear that neglecting y does not affect the optimum while in the case of high AR both degrees of freedom are involved in the generation of moment and in this case neglecting a degree of freedom is less advantageous but imposing a fixed y position at the average value it is possible to obtain a technologically advantageous solution with a behaviour very close to the optimal one.
As a proof of concept **Figure 12** compares the results obtained for an ideally rigid wing of aspect ratio $\lambda=26$ with a 2-dof optimization and a 1-dof optimization imposing the rib position at an average value calculated from the 2-dof optimization.

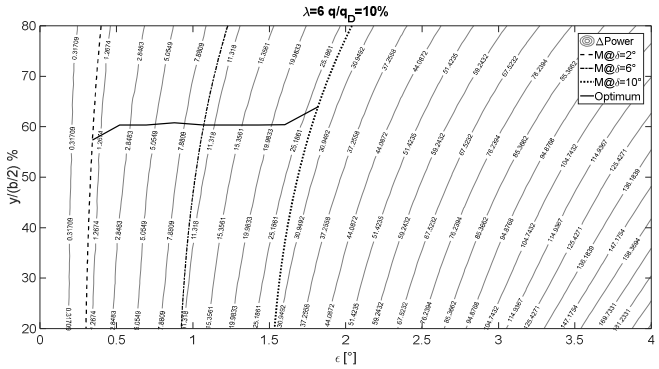

Figure 10 Low λ: Rolling moment constraint and iso-ΔP lines.

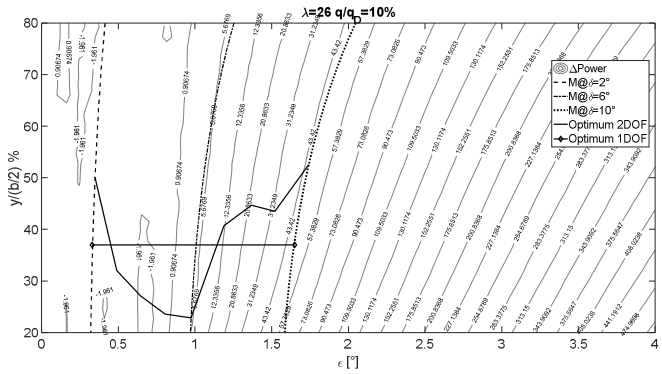

Figure 11 High λ: Rolling moment constraint and iso-ΔP lines with 1 and 2 DOF optimums

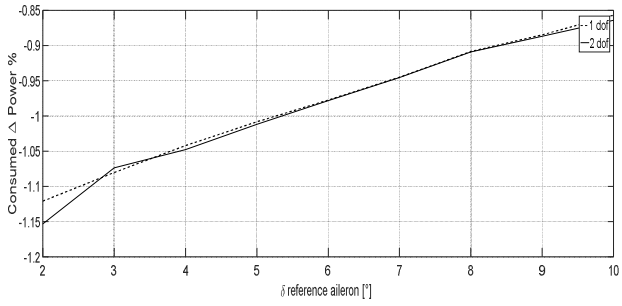

Figure 12 DOF comparison

4. Conclusions

The paper present the results obtained from the analysis of a warping solution for the generation of a rolling moment equivalent to a classical solution with ailerons. An optimization analysis was presented in order to reduce the aerodynamic power necessary for generating the desired rolling moment. The proposed solution presents two degree of freedom corresponding to the actuation rib position and warping angle.

The analysis showed that the morphing solution is very advantageous in all cases requiring high rolling moments where advantage of more than 50% respect to the conventional solution has been obtained. A more evident advantage is obtained at high aspect ratios. The traditional solution still remain advantageous at low aspect ratios and low rolling moments.

The effect of flexibility is also considered and its effect result dominant when low rolling moment is required. At high rolling moments the effect of flexibility can be considered a secondary effect respect to the drag increase produced by the aileron deflection.

5. References

1. A.Y.N. Sofla, S.A. Meguid, K.T. Tan, W.K. Yeo. Shape morphing of aircraft wing: Status and challenges, Materials and Design 31 (2010) 1284–1292.

2. R. Pecora, F. Amoroso, and L. Lecce, Effectiveness of Wing Twist Morphing in Roll Control, Journal of Aircraft vol. 49, no. 6, November–December 2012

3. R. M. Ajaj, M. I. Friswell, W. G. Dettmer, A. T. Isikveren and G. Allegri, Roll control of a MALE UAV using the adaptive torsion wing, The Aeronautical Journal March 2013 Volume 117 No 1189

4. Mujahid Abdulrahim, Helen Garcia and Rick Lind, Flight Characteristics of Shaping the Membrane Wing of a Micro Air Vehicle JOURNAL OF AIRCRAFT Vol. 42, No. 1, January–February 2005

5. Bret Stanford, Mujahid Abdulrahim, Rick Lind,† and Peter Ifju, Investigation of Membrane Actuation for Roll Control of a Micro Air Vehicle JOURNAL OF AIRCRAFT Vol. 44, No. 3, May–June 2007

6. Frulla, Giacomo; Cestino, Enrico; Gili, Piero; Visone, Michele; Scozzola, Domenico (2015), A Possible Adaptive Wing Apparatus for New UAV Configurations., SAE 2015 AeroTech Congress & Exibition, Seatle (WA-USA), 22-25 September 2015.

7. Gili, Piero; Frulla, Giacomo (2016) A variable twist blade concept for more effective wind generation: design and realization,
In: SMART SCIENCE, pagine 78-86, ISSN: 2308-0477.
8. FRULLA G.; CESTINO E. (2014) Analysis of slender thin-walled anisotropic box-beams including local stiffness and coupling effects,
In: AIRCRAFT ENGINEERING AND AEROSPACE TECHNOLOGY, pag. 345-355, ISSN: 1748-8842
9. MARTINEZ, JOAN MARC; SCOPELLITI, DOMENICO; BIL, CEES; CARRESE, ROBERT; MARZOCCA, PIER; CESTINO, ENRICO; FRULLA, GIACOMO. Design, Analysis and Experimental Testing of a Morphing Wing - (2017). 25th AIAA/AHS Adaptive Structures Conference, Grapevine, Texas, 9-13 January 2017.

Copyright Statement

Contact Author Email address

The corresponding author can be contacted at the following email addresses: enrico.cestino@polito.it